Journal of Sound and Vibration (1999) **225**(1), 111–126
Article No. jsvi.1999.2237, available online at http://www.idealibrary.com on IDEAL®

ON THE MECHANISMS OF VIBRATIONAL INSTABILITY IN A CONSTRAINED ROTATING STRING

JIFANG TIAN AND STANLEY G. HUTTON
Department of Mechanical Engineering, UBC, Vancouver, BC, V6T 1Z4, Canada

(*Received* 1 *December* 1997, *and in final form* 17 *February* 1999)

A relatively simple mathematical model involving an idealized rotating string constrained at one point is used to develop an understanding of the basic physical mechanisms that govern the development of unstable lateral vibration response. Equations defining the relationship between the interactive inertial, damping, elastic and applied forces are presented. Analysis of these equations leads to a clear understanding of the physical mechanisms involved in the development of divergence and flutter instability mechanisms. New developments involve the identification of the energy flux into the rotating system and an explanation of the role of circumferential forces caused by interaction with the non-rotating constraint. The equations developed suggest methods for minimizing the instability regions that are encountered in such rotating systems when operating above their lowest critical speed. Numerical examples are presented for the case of a rotating string to illustrate its instability characteristics when constrained by a single degree of freedom viscously damped system.

1. INTRODUCTION

Often, rotating machinery contains components that are high-energy systems with latent instabilities. Under certain circumstances, the driving energy in such systems can be channelled into lateral vibration modes leading to unstable behavior. In order to prevent such energy transmission, an understanding of these instability mechanisms is required.

The essential physical mechanisms involved in rotor system instabilities have been studied by Crandall [1, 2] through the use of simplified models. However, the physical mechanisms involved in rotating systems with transverse vibration are not well understood, especially for instability mechanisms caused by the interaction with stationary components. These mechanisms are involved in a broad range of problems involving rotor/stator interaction of greater complexity than the model considered in this paper. Such problems are encountered in turbine disks, computer floppy discs and guided saw blades for example. Mote [3, 4], Chen *et al.* [5, 6], Iwan and Moeller [7] and many other researchers have presented mathematical analyses that predict the onset of instability for a rotating disk-stationary load system or for a stationary disk with a moving load system.

0022-460X/99/310111 + 16 $30.00/0

However, these studies do not make clear the physical mechanisms responsible for the onset of these instabilities. Shen and Mote [8] presented a physical explanation of the instability mechanisms of a stationary circular plate subjected to a rotating damped spring–mass system and Yang and Hutton [9] presented a physical explanation of the instability of a rotating circular string due to interaction with a stationary frictional force. However, clear physical explanations for the development of such instabilities in general are lacking.

The purpose of this paper is to investigate the instability mechanisms that are involved in the interaction between a rotating string an an interactive stationary system with elastic, inertial, and damping characteristics together with a general non-conservative force. New developments presented in this work include the definition of the energy flux into the rotating system and the identification of circumferential forces caused by the interaction with the non-rotating constraint. Exact equations defining the relationship between the interactive forces and energy flux are derived, which lead to a clear understanding of the physical mechanisms involved in the development of divergence and flutter instability mechanisms. On the basis of these equations, methods for minimizing the instability regions for the model under consideration are discussed.

The present paper is an extension of the work presented as a technical note [10].

2. THEORETICAL BACKGROUND

Figure 1 shows a circular string of radius r, rotating at a constant angular velocity Ω, attached to a stationary spring-mass-dashpot system at $(r, \theta = 0)$ with no friction being generated by the motion of the string with respect to the constraint. The governing equation of transverse motion $u(\theta, t)$, with respect to stationary coordinates, and its displacement and force boundary conditions can be

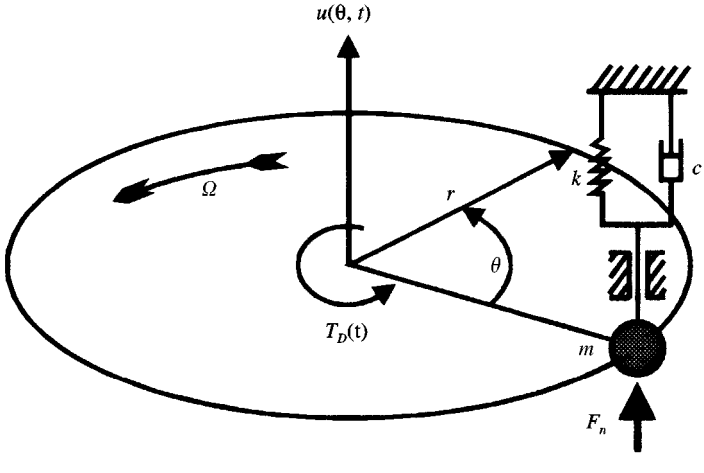

Figure 1. A rotating string subjected to stationary interactive forces.

expressed as [9]

$$u_{,tt} + 2\Omega u_{,\theta t} - \left(\frac{P}{\rho r^2} - \Omega^2\right) u_{,\theta\theta} = 0, \quad u(0, t) - u(2\pi, t) = 0, \tag{1, 2}$$

$$(S^2 - \Omega^2)[u_{,\theta}(2\pi, t) - u_{,\theta}(0, t)] + \frac{k}{\rho r} u(0, t) + \frac{m}{\rho r} u_{,tt}(0, t) + \frac{c}{\rho r} u_{,t}(0, t) - \frac{1}{\rho r} F_n(0, t) = 0, \tag{3}$$

where $S^2 = P/(\rho r^2)$; S, P and ρ are flexural wave speed, string tension (assumed constant) and density per unit length, respectively; k, c, and m are the stiffness, damping and mass parameters, respectively, of the constraint system; $F_n(0, t)$ represents an arbitrary non-conservative force produced by the stationary system in the transverse direction. For small displacements, the potential energy PE and the kinetic energy TE of the total system can be written as

$$PE = \int_0^{2\pi} \tfrac{1}{2} P \left(\frac{u_{,\theta}}{r}\right)^2 r \, \mathrm{d}\theta + \tfrac{1}{2} k u^2(0, t), \tag{4}$$

$$TE = \int_0^{2\pi} \tfrac{1}{2} \rho [\Omega^2 r^2 + (u_{,t} + \Omega u_{,\theta})^2] r \, \mathrm{d}\theta + \tfrac{1}{2} m u_{,t}^2(0, t), \tag{5}$$

Then the rate of the change of total energy (power) $E_{,t}$ is given by

$$E_{,t} = PE_{,t} + TE_{,t}. \tag{6}$$

Substituting equations (4) and (5) into equation (6) and simplifying the result using the governing equation and the boundary conditions yields the equation (the detailed derivation is given in Appendix A):

$$E_{,t} = \Omega(F_k + F_m + F_c + F_n)\bar{u}_{,\theta}(0, t) + F_c u_{,t}(0, t) + F_n u_{,t}(0, t), \tag{7}$$

where $F_k = -ku(0, t)$, $F_m = -mu_{,tt}(0, t)$ and $F_c = -cu_{,t}(0, t)$ are the lateral elastic, inertial and viscous damping forces acted on the string, caused by the constraint at the location $(r, \theta = 0)$; $\bar{u}_{,\theta}(0, t)/r = [u_{,\theta}(2\pi, t) + u_{,\theta}(0, t)]/(2r)$ is the average slope of the string at the constraint location. Note that equation (7) is an exact expression derived from the exact solution of the string motion, which can also be rewritten in the following forms:

$$\begin{aligned} E_{,t} &= -\Omega r(F_{\theta k} + F_{\theta m} + F_{\theta c} + F_{\theta n}) + F_c u_{,t}(0, t) + F_n u_{,t}(0, t) \\ &= -\Omega(T_k + T_m + T_c + T_n) + F_c u_{,t}(0, t) + F_n u_{,t}(0, t) \end{aligned} \tag{8}$$

or

$$E_{,t} = \Omega T_D(t) + F_c u_{,t}(0, t) + F_n u_{,t}(0, t), \tag{9}$$

where $F_{\theta k} = -F_k \operatorname{tg}\alpha = -F_k(\bar{u}_{,\theta}/r)$, $F_{\theta m} = -F_m(\bar{u}_{,\theta}/r)$, $F_{\theta c} = -F_c(\bar{u}_{,\theta}/r)$ and $F_{\theta n} = -F_n(\bar{u}_{,\theta}/r)$ are the circumferential components of the interactive forces acted on the string. The torques produced by these circumferential components can be expressed as $T_k = F_{\theta k} r$, $T_m = F_{\theta m} r$, $T_c = F_{\theta c} r$ and $T_n = F_{\theta n} r$.

Figure 2 illustrates the forces involved for the case where the constraint consists only of a stiffness component. As the string–spring interface is assumed frictionless, the spring applies a normal force R to the deflected rotating string. The vertical component of this force F_k must balance the spring force $ku(0, t)$, whereas the horizontal component of this force $F_{\theta k}$ will result in a torque $F_{\theta k} r$ applied to the string. This torque must be provided by the driving torque T_D in order for the system to rotate at constant speed. Thus, in the general case where inertial, damping, stiffness and non-conservative forces exist at the constraint interface the driving torque T_D must supply a torque that exactly balances the sum of the individual torques in order to maintain motion at constant speed. One implication of this result is that the applied torque required to produce constant speed is not constant. Under these assumptions, it can be seen from equation (9) that the work done by lateral interactive force F_k is equal to the work done by the driving torque T_D. Therefore, if the work done by T_D is greater than zero over a complete cycle of motion, the driving energy will be channelled into vibration energy and unstable behavior will result.

To analyze the energy flux in this system, equation (9) can be expressed in the form

$$\Delta E = \int_0^\tau [N_{Ik} + N_{Im} + (N_{Ic} - N_{oc}) + (N_{In} - N_{on})]\, \mathrm{d}t, \tag{10}$$

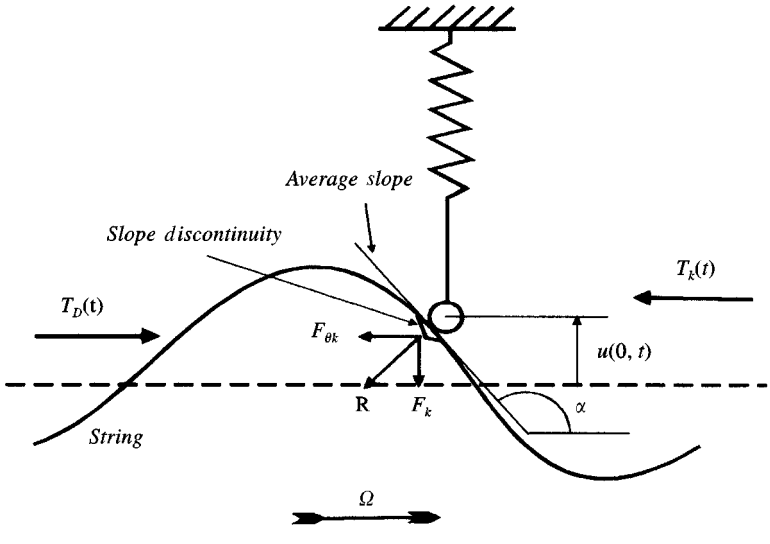

Figure 2. Interactive forces applied to the rotating string due to a spring constraint, $\tan(\alpha) = \bar{u}_{,\theta}/r$.

where ΔE represents the change of total energy in the system during the time interval $0 \sim \tau$; $N_{Ik} = -T_k\Omega$, $N_{Im} = -T_m\Omega$, $N_{Ic} = -T_c\Omega$ and $N_{In} = -T_n\Omega$ are the components of the input power provided by the driving torque; and $N_{oc} = cu_{,t}^2(0, t)$ and $N_{on} = -F_n u_{,t}(0, t)$, represent the power dissipated by a viscous damper and a non-conservative force. Thus, the resultant power into the system through these non-conservative elements are $N_{Ic} - N_{oc}$ and $N_{In} - N_{on}$ respectively.

From equation (10) it should be noted that if the total energy of this system increases, as the rotational speed is constrained to be constant, the driving energy for the steady rotation will be transferred into lateral vibration, i.e., unstable behavior will occur. Thus, equation (10) is the basic relationship that provides physical insight into the stability characteristics of the system. Under stable conditions, ΔE will be a non-zero function of time, but over a sufficiently long period its mean value will be zero. For unstable conditions, ΔE will increase without limit for suitably high τ. The manner in which ΔE changes will depend upon the initial conditions and the specific constraint applied. If, for example, the initial conditions do not contain a significant contribution of an unstable mode the time required for the instability to show itself will be longer than in the case where the initial conditions contained a significant component of the unstable mode.

In the present paper, the response of the system will be considered in terms of two of its modes. The generalization to greater numbers of modes is straightforward.

If no interactive system is present, i.e., $k = m = c = F_n(0, t) = 0$, the system is always stable.

3. DIVERGENCE INSTABILITY

Divergence is a standing wave instability and can occur at a critical speed of a rotating system. This type of instability can be mathematically defined as a state in which the real part of one of the system eigenvalues $\sigma_n > 0$ and the imaginary part $\omega_n = 0$. Such instabilities are to be found in rotating disc interaction problems [3–7].

Divergence instability cannot occur in the present model. When the rotating speed Ω equals the wave speed S, the backward-wave mode shape appears as a stationary wave for an unconstrained string system when observed from fixed co-ordinates. It can be noted from equation (3) that divergence instability cannot occur at the wave speed in the constrained rotating string system because the total interactive forces between the string and constraint become zero when $\Omega = S$, which means that $\Delta E(t) = 0$. At a rotational speed corresponding to the wave speed a standing wave can occur and this can be associated with a resonant condition in the case where the string is subjected to a constant lateral force. This resonance does not correspond to an instability which is characterized by a system eigenvalue having a positive real part.

4. FLUTTER INSTABILITY

Flutter is a type of dynamic instability characterized by oscillations with increasing amplitude, and for a rotating string subjected to stiffness, mass and damping

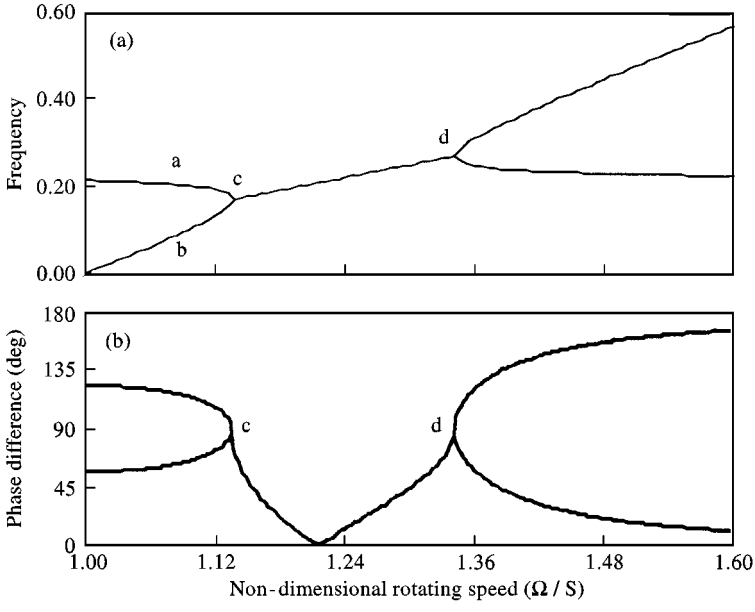

Figure 3. Response characteristics due to stiffness constraint ($k' = kr/P = 1{\cdot}0$). (a) Natural frequency, (b) phase difference $\Delta\varphi_{ij}$ between interactive force and $\bar{u}_{,\theta}(0, t)$.

constraints it occurs at supercritical speeds, i.e. in the present study at speeds above the wave speed. Mathematically, flutter instability can be defined as a state in which the real part of a system eigenvalue $\sigma_n > 0$ and the imaginary part $\omega_n > 0$. This type of instability always occurs as a result of the coupling of two vibratory modes in a given speed region. The onset of the flutter is characterized by the coincidences of mode frequencies and mode shapes. The coupled modes subsequently separate after some increase in rotating speed as shown in Figure 3(a).

Consider first the case of a stiffness constraint. The total energy change of two modes i and j can be expressed as

$$\Delta E = \Omega \int_0^\tau (F_{ki} + F_{kj})(\bar{u}_{,\theta i} + \bar{u}_{,\theta j})\,\mathrm{d}t \tag{11}$$

or

$$\Delta E = -\Omega r \int_0^\tau (F_{\theta kii} + F_{\theta kij} + F_{\theta kji} + F_{\theta kjj})\,\mathrm{d}t = \Delta E_{ii} + \Delta E_{ij} + \Delta E_{ji} + \Delta E_{jj}, \tag{12}$$

where

$$\Delta E_{ii} = -\Omega \int_0^\tau F_{\theta kii} r\,\mathrm{d}t = \Omega r \int_0^\tau F_{ki}(\bar{u}_{,\theta i}/r)\,\mathrm{d}t,$$

$$\Delta E_{jj} = -\Omega \int_0^\tau F_{\theta kjj} r\,\mathrm{d}t = \Omega r \int_0^\tau F_{kj}(\bar{u}_{,\theta j}/r)\,\mathrm{d}t,$$

$$\Delta E_{ij} = -\Omega \int_0^\tau F_{\theta kij} r \, \mathrm{d}t = \Omega r \int_0^\tau F_{ki}(\bar{u}_{,\theta j}/r) \, \mathrm{d}t,$$

$$\Delta E_{ji} = -\Omega \int_0^\tau F_{\theta kji} r \, \mathrm{d}t = \Omega r \int_0^\tau F_{kj}(\bar{u}_{,\theta i}/r) \, \mathrm{d}t.$$

ΔE_{ii} and ΔE_{jj} represent the energy changes caused by the circumferential force components $F_{\theta kii}$ and $F_{\theta kjj}$ of the $i(j)$th modes, respectively. ΔE_{ij} and ΔE_{ji} represent the energy changes due to the action of the coupled circumferential force components $F_{\theta kij}$ and $F_{\theta kji}$, respectively.

It can be proven [9] that in the absence of damping the phase difference between the displacement $u_i(0, t)$ and the average slope $\bar{u}_{\theta i}(0, t)$ for a single mode is always 90° in an uncoupled region. ΔE_{ii} is thus given by

$$\Delta E_{ii} = \Omega \int_0^\tau F_{ki} \bar{u}_{,\theta i}(0, t) \, \mathrm{d}t = -k\Omega \int_0^\tau u_i(0, t) \bar{u}_{,\theta i}(0, t) \, \mathrm{d}t$$

$$= A_{ii}(\Omega) \int_0^\tau \sin[\omega_i(\Omega)t + \varphi_i(\Omega) + \pi] \sin[\omega_i(\Omega)t + \varphi_i(\Omega) + \pi/2] \, \mathrm{d}t, \qquad (13)$$

where the magnitude $A_{ii}(\Omega)$, angular frequency $\omega_i(\Omega)$ and phase angle $\varphi_i(\Omega)$ are all functions of the rotating speed Ω.

ΔE_{ii} is a periodic function of time with zero mean, which implies that there is only a periodically oscillating energy flow into and out of the system. This means that flutter instability due to a stationary stiffness cannot occur in a single mode by itself. In this case, the circumferential force component $F_{\theta kii}$ is also a periodic function of time, so a periodic driving torque that does zero-mean work is required to balance $F_{\theta kii}$ in order to keep the system rotating at constant speed.

Consider now two modes with different frequencies ω_{ia} and ω_{jb}, that are approaching each other as shown in Figure 3(a); the coupling terms ΔE_{ij} and ΔE_{ji} that are responsible for the flutter instability of the system can be expressed as

$$\Delta E_{ij} = \Omega \int_0^\tau F_{ki} \bar{u}_{,\theta j}(0, t) \, \mathrm{d}t = A_{ij}(\Omega) \int_0^\tau \sin[\omega_{ia}(\Omega)t + \varphi_{ia}(\Omega)] \sin[\omega_{jb}(\Omega)t + \varphi_{jb}(\Omega)] \, \mathrm{d}t, \qquad (14)$$

where $\varphi_{ia}(\Omega)$ and $\varphi_{jb}(\Omega)$ are the phase angles associated with the stiffness force of the ith mode and with the mean slope of the jth mode respectively. It can be verified that ΔE_{ij} is a periodic function with zero mean when $\omega_{ia} \neq \omega_{jb}$, which implies that flutter instability due to a stationary stiffness cannot occur in two modes with different frequencies. The circumferential force component $F_{\theta kij}$ is also a periodic function with zero mean when the ith and jth modes have different frequencies.

As shown in Figure 3(a), when the two modes become coupled at point c, the frequencies of the coupled modes become identical, and the phase difference $\Delta\varphi_{ij}$ between the elastic force F_{ki} and the slope $\bar{u}_{,\theta j}(0, t)$ becomes 90°. At this point the total energy change is still periodic with zero mean. In the flutter region, the coupled modes have identical frequencies and mode shapes. In this case, the phase difference $\Delta\varphi_{ii}$ between F_{ki} and $\bar{u}_{,\theta i}(0, t)$ varies from 90° at point c to 0° at some rotational speed in the flutter area, it then returns to 90° at point d as shown in Figure 3(b). These results were obtained from the exact solution of the free response analysis of the string system.

It can be proven mathematically that ΔE_{ij} is an increasing positive oscillatory function of time when $\omega_{ia} = \omega_{jb}$ and $0 \leqslant \Delta\varphi_{ii} < 90°$. In this case, the circumferential component $F_{\theta kii}$ caused by the two coupled modes is a periodically oscillating increasing function of time with a positive mean, so a corresponding driving torque that does positive work is required to balance it. Without any energy dissipation, the system becomes unstable.

For the case of a mass constraint, the circumferential component $F_{\theta mii}$ that is caused by two coupled modes is also periodic with positive mean when $0 \leqslant \Delta\varphi_{ii} < 90°$, so a corresponding driving torque is required to balance the circumferential force, which leads to a positive energy flux into the system.

The preceding arguments also apply to the case of simultaneous mass and stiffness constraints, in which case the circumferential component is $F_{\theta k} + F_{\theta m}$. Figure 4 shows the flutter region caused by the circumferential force $F_{\theta k} + F_{\theta m}$ and the phase difference between the total interactive force $F_k + F_m$ and the slope $\bar{u}_{,\theta}(0, t)$. It is noted that the phase difference is such that $0 \leqslant \Delta\varphi_{ii} < 90°$ in the flutter region.

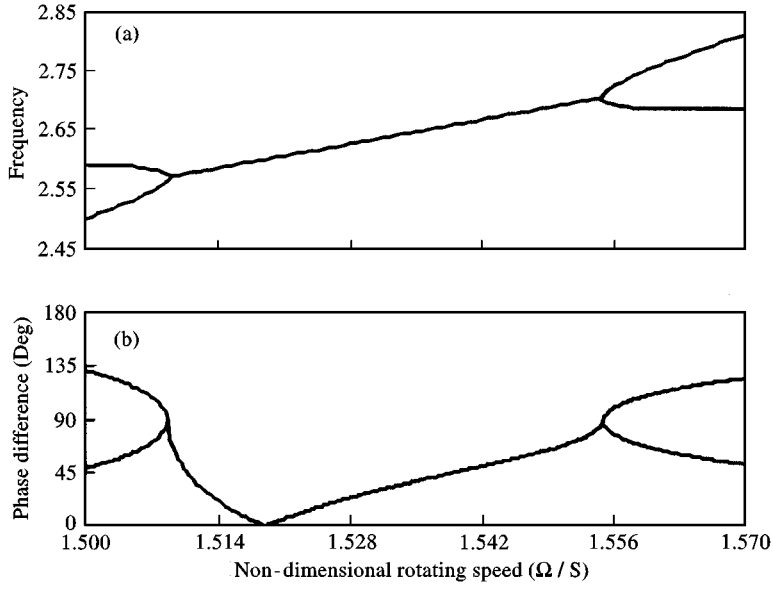

Figure 4. Response characteristics due to mass constraint [$m' = m/(\rho r) = 0{\cdot}3$] and stiffness constraint ($k' = 3{\cdot}0$). (a) Natural frequency, (b) phase difference $\Delta\varphi_{ij}$.

From equations (7) and (8), it can be noted that for the case of simultaneous mass and stiffness constraints flutter instability will disappear when $F_{\theta k} + F_{\theta m} = -(F_k + F_m)\bar{u}_{,\theta}(0, t)/r = 0$. Within the flutter region, the total circumferential force generated by the mass and stiffness constraints is given by

$$F_{\theta k} + F_{\theta m} = m(\omega_0^2 - \omega_i^2)u(0, t)\bar{u}_{,\theta}(0, t)/r, \tag{15}$$

where $\omega_0^2 = k/m$; ω_i is some frequency in the flutter region. Therefore, the flutter instability can be minimized by setting $\omega_0^2 = \bar{\omega}_i^2$, where $\bar{\omega}_i$ is an average frequency for the flutter region. Figures 5 and 6 illustrate four flutter instability regions before and after such a modification is made. The effect on minimizing the flutter regions can clearly be seen in Figure 6. The flutter regions reduce or even disappear and the real parts of the eigenvalues are notably diminished due to a significant reduction of the resultant circumferential force.

Note also that, for the case of stiffness constraints, a particular flutter region may be eliminated or minimized by putting two springs at appropriate locations on the string in order that

$$F_{\theta k} = [k_1 u(\theta_1, t)\bar{u}_{,\theta}(\theta_1, t) + k_2 u(\theta_2, t)\bar{u}_{,\theta}(\theta_2, t)] = 0, \tag{16}$$

where θ_1 and θ_2 represent two specific positions on the string. The system may then become more stable because the interactive circumferential force that causes positive energy flow into the system has been minimized.

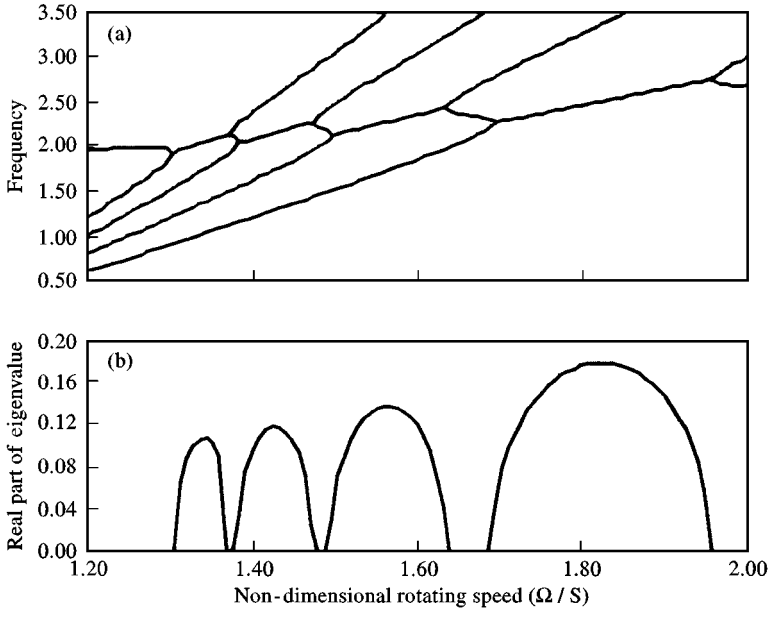

Figure 5. Response characteristics for mass constraint ($m' = 0{\cdot}6$); (a) frequency, (b) real part of eigen value.

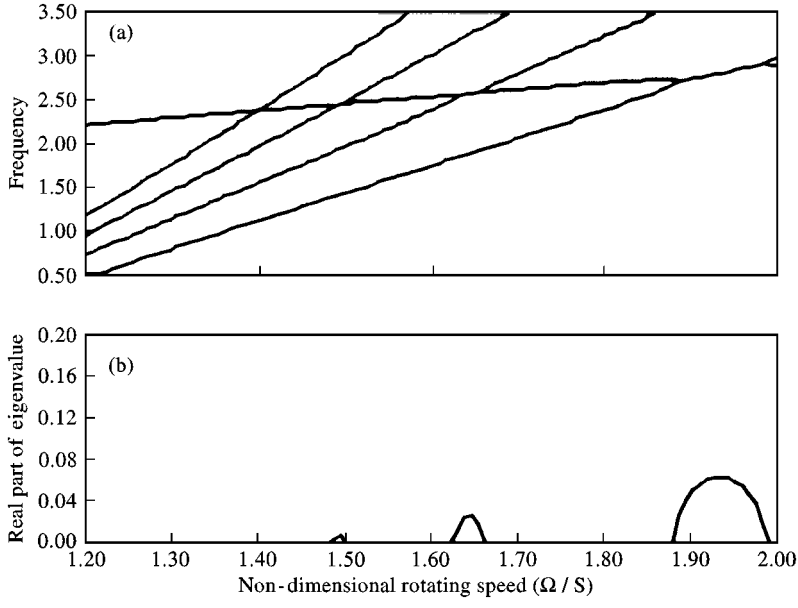

Figure 6. Response characteristics for combined mass ($m' = 0{\cdot}6$) and stiffness constraints ($k' = 3{\cdot}31$, $\bar{\omega}_i = 2{\cdot}35$). (a) frequency, (b) real part of eigenvalue.

If the present system were analyzed with respect to axes moving at the rotational speed of the string the flutter instabilities of the present analysis would appear as parametric instabilities.

5. TERMINAL FLUTTER INSTABILITY

A special type of flutter instability which occurs at all speeds above a particular rotating speed is termed "terminal instability". The occurrence of terminal flutter usually involves a single mode and a non-conservative force. A typical example of this type of instability is the flutter instability caused by a constraint consisting of a stationary viscous damper. Figure 7 illustrates the effect of viscous damping on the eigenvalues of a rotating string, where modes nF and nR represent forward and reflected travelling wave modes with n nodal diameters.

From Figure 7(a), it is noted that the frequencies of the system are similar to those in a system without a constraint, with all the frequency curves going through the crossing points without coupling. From Figure 7(b), however, it can be noted that all the backward reflected wave modes become unstable at supercritical speeds and the instability involves a single mode. At supercritical speeds the real parts of the eigenvalues for reflected waves increase almost linearly with rotating speed but they reduce to zero when the reflected wave modes meet the forward wave modes. It can also be noted that the real parts of the eigenvalues for the forward wave modes have negative values and decrease linearly except near crossing points where they all take a common value. Thus, the forward wave modes associated with a stationary viscous damper constraint are always stable.

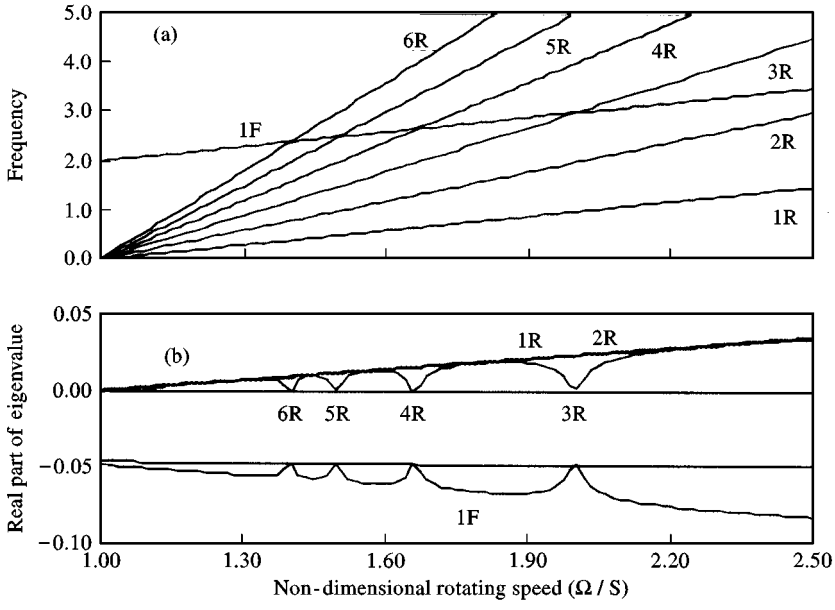

Figure 7. Response characteristics due to viscous damper constraint ($c' = c/\sqrt{\rho P} = 0{\cdot}3$). (a) Natural frequencies at supercritical speeds, (b) real parts of eigenvalues.

The resultant energy change in the system for a stationary damping constraint can be expressed [using equations (7) and (9)] as

$$\Delta E = \int_0^\tau [\Omega F_c \bar{u}_{,\theta}(0, t) - c u_{,t}^2(0, t)]\, \mathrm{d}t = \int_0^\tau [\Omega T_{Dc} - c u_{,t}^2(0, t)]\, \mathrm{d}t \tag{17}$$

or

$$\Delta E = \int_0^\tau [F_c u'_{,t}(0, t)]\, \mathrm{d}t, \tag{18}$$

where $u'_{,t}(0, t) = u_{,t}(0, t) + \Omega \bar{u}_{,\theta}(0, t)$, which is the relative transverse velocity at the constraint observed from rotating co-ordinates, while $u_{,t}(0, t)$ represents the absolute transverse velocity at the constraint observed from fixed co-ordinates. From equation (17), it is noted that the energy into the system equals the difference between the total input energy required to overcome the torque induced by the damper force and the energy dissipated by the same damper.

The total input energy ΔE_i introduced by the ith reflected wave mode is given by

$$\Delta E_i = \Omega \int_0^\tau F_c \bar{u}_{,\theta}(0, t)\, \mathrm{d}t = A_{ii}(\Omega) \int_0^\tau \sin(\omega_{ii} t + \varphi_{Fi}) \sin(\omega_{ii} t + \varphi_{\alpha i})\, \mathrm{d}t, \tag{19}$$

where φ_{Fi} and $\varphi_{\alpha i}$ are the phase angles of F_c and $\bar{u}_{,\theta}(0, t)$, respectively.

The phase differences $\Delta\varphi_{F\alpha}$ between F_c and $\bar{u}_{,\theta}(0, t)$ for modes 1R(1B) and 4R(4B) are calculated and the results are shown in Figure 8. From Figure 8 it can be seen

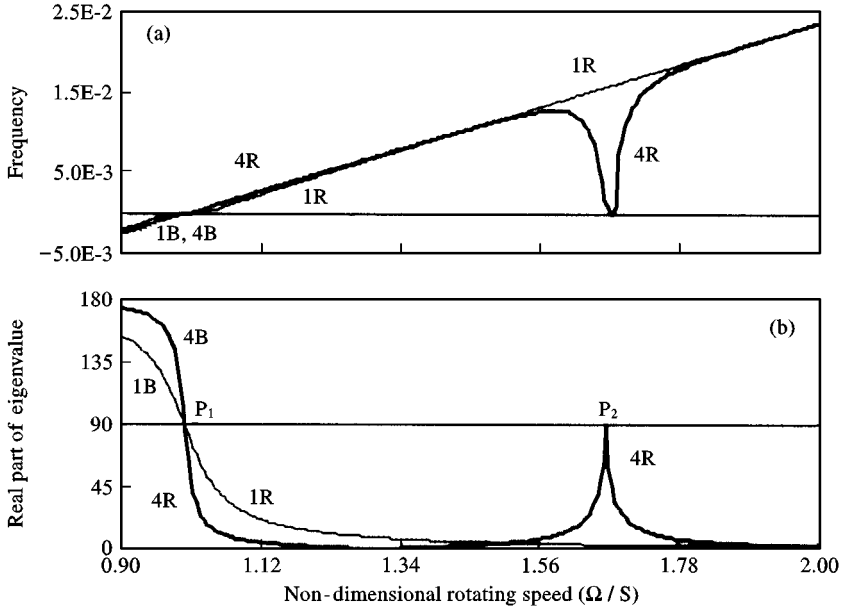

Figure 8. Response characteristics due to viscous damper constraint ($c' = 0{\cdot}3$). (a) Real parts of eigenvalues for modes 1B and 4B, (b) phase difference $\Delta\varphi_{F\alpha}$.

that F_c is always out of phase with $\bar{u}_{,\theta}(0, t)$ at subcritical speeds and in phase with $\bar{u}_{,\theta}(0, t)$ at supercritical speeds. As a result, energy is removed from the system at subcritical speeds (P_1) but is input into the system at supercritical speeds except at the speed corresponding to the crossing point (P_2). It can be noted that $\Delta\varphi_{F\alpha}$ at the crossing point (P_2) becomes 90°. Therefore, the periodic energy flux into the system has zero mean and this mode becomes stable at the crossing points.

Figure 9 schematically illustrates the effects of a viscous damper on the backward wave mode instability. In Figure 9 the solid curve is the backward wave observed in fixed co-ordinates at supercritical speeds and the dashed curve represents the backward wave observed in the co-ordinates rotating with the string. From this figure it can be seen that the transverse damping force F_c is always in phase with the average slope $\bar{u}_{,\theta}(0, t)/r$ at the constraint on the solid curve at supercritical speed, i.e., $F_c < 0$ and $\bar{u}_{,\theta}(0, t) < 0$ at the position shown in Figure 9. Therefore, the energy introduced by the damper ΔE_I is always greater than zero, which implies that the driving energy is switched into the vibratory energy of the reflected wave mode through the damper.

According to equation (18), the net energy change of the system equals the work done by the damping force F_c with the relative wave velocity $u'_{,t}(0, t)$ indicated by the dash curve. It should be noted that F_c only depends on $u_{,t}(0, t)$ which is dependent on the rotating speed of the string, while $u'_{,t}(0, t)$ is independent of rotating speed. It can be seen that F_c is in phase with $u'_{,t}(0, t)$ at supercritical speed. Thus, F_c does positive work on the reflected wave and destabilizes its motion. It can also be shown that F_c is always out of phase with $\bar{u}_{,\theta}(0, t)$ or $u'_{,t}(0, t)$. Therefore, the damper always stabilizes the backward wave at subcritical speeds. For the forward

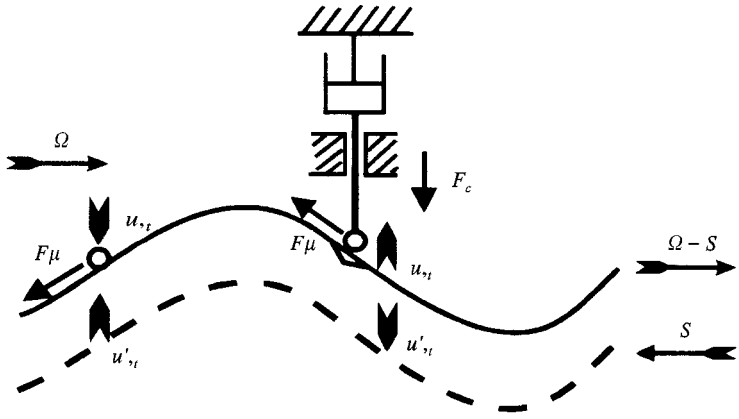

Figure 9. Backward-wave mode instability due to viscous damper constraint or friction (——, observed in space-fixed co-ordinates; – – –, observed in string-fixed co-ordinates).

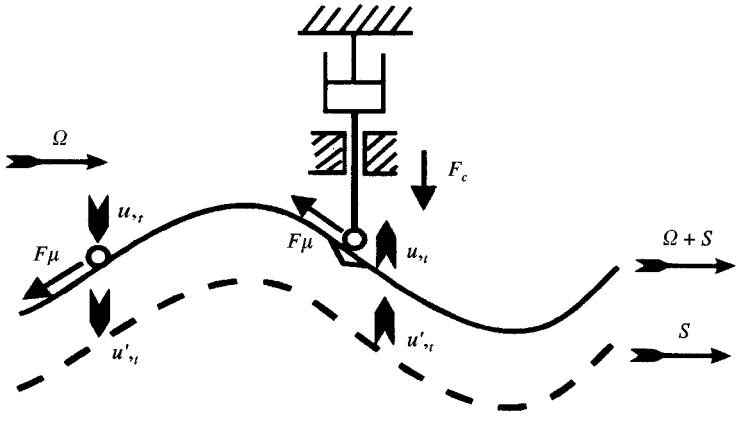

Figure 10. Forward-wave mode instability due to viscous damper constraint or friction (—— observed in space-fixed co-ordinates; – – –, observed in string-fixed co-ordinates).

wave shown in Figure 10, it can be seen that F_c is always out of phase with $u'_{,t}(0, t)$. As a result, the damper stabilizes the forward wave mode at all speeds.

From Figures 9 and 10, it can also be seen that in the case of friction the lateral component of F_μ is always out of phase with $u'_{,t}(0, t)$ for the backward wave mode and is always in phase with $u'_{,t}(0, t)$ for the forward wave mode, regardless of rotating speed. Therefore, stationary friction stabilizes the backward wave mode and destabilizes the forward wave mode at all speeds. This result agrees with the theoretical eigenvalue analysis [9].

The above illustration also applies to the case where the constraint is an arbitrary non-conservative force F_n. The net energy into the system can be expressed from equation (7) as

$$\Delta E = \int_0^\tau F_n[u_{,t}(0, t) + \Omega \bar{u}_{,\theta}(0, t)\,\mathrm{d}t = \int_0^\tau F_n u'_{,t}(0, t)\,\mathrm{d}t, \tag{20}$$

In this case, the stability of the system relies on the characteristics of F_n.

6. CONCLUSIONS

In this study, the relationship between energy flux and the interactive forces for an idealized constrained string rotating at constant speed has been derived. This equation leads to a clear understanding of the physical mechanisms involved in the development of vibrational instabilities in this system. The instability mechanisms identified in this work can be expected to have relevance in the understanding of the behavior of more complex systems.

(1) The circumferential component of the interactive force between the stationary constraint and the rotating string is a primary factor in all instability mechanisms.

(2) When the interactive force applied to the rotating string is in phase with the average slope $\bar{u}_{,\theta}(0, t)/r$ at the constraint, driving energy will be switched into vibratory energy leading to unstable behavior. In this case, the circumferential component of the interactive force has a positive mean value. Vibratory energy will be switched back into driving energy when the interactive force is no longer in phase with $\bar{u}_{,\theta}(0, t)$. At this time the circumferential component of the interactive force has a negative mean value.

(3) When the phase difference between the interactive force and $\bar{u}_{,\theta}(0, t)$ is 90° there is a periodically oscillating energy flow into and out of the system, in which case, the total energy of the system is periodic function of time with zero mean.

(4) In the constrained rotating string divergence instability cannot occur at the critical speed because the constraint forces must sum to zero as the string tension and inertia effects cancel. Under such conditions no energy can be input into the system.

(5) Flutter instability only occurs with stationary stiffness and mass constraints at supercritical speeds. Terminal flutter instability occurs at supercritical speeds in conjugation with non-conservative interactive forces. A stationary viscous damper, for example, can not only dissipate vibratory energy but can also introduce net energy into the system at supercritical speeds leading to the possibility of terminal flutter instability.

(6) The severity of the instability in a given flutter region can be minimized by choosing appropriate stationary stiffness and mass charcteristics or by positioning constraints at locations that minimize the circumferential force.

REFERENCES

1. S. H. Crandall 1983 *Rotor Dynamic Instability*, *The Applied Mechanics, Bioengineering and Fluids Engineering Conference*, *Houston*, *Texas*, 20–22 *June* 1983, 1–18. The physical nature of rotor instability mechanism.
2. S. H. Crandall 1990 *Dynamical Problems of Rigid-Elastic Systems and Structures*, *IUTAM Symposium*, *Moscow*, *USSR*, 65–72. Stability of vibratory modes in moving media.
3. C. D. Mote 1970 *Journal of Franklin Institute* **290**, 329–344. Stability of circular plates subjected to moving loads.
4. C. D. Mote 1977 *Journal of the Accoustical Society of America* **61**, 439–447. Moving-load stability of a circular plate on a floating central collar.

5. K. Ono, J. S. Chen, and D. B. Bogy 1991 *ASME Journal of Applied Mechanics*, **58**, 1005–1014. Stability analysis for the head–disk interface in a flexible disk drive.
6. J. S. Chen and D. B. Bogy 1992 *ASME Journal of Applied Mechanics*, **59**, 230–235. Effects of load parameters on the natural frequencies and stability of a flexible spinning disk with a stationary load system.
7. W. D. Iwan and T. L. Moeller 1976 *ASME Journal of Applied Mechanics*, **43**, 485–490. The stability of a spinning elastic disk with a transverse load system.
8. I. Y. Shen and C. D. Mote Jr. 1991 *Journal of Sound and Vibration* **148**, 307–318. On the mechanism of instability of a circular plate under a rotating spring–mass–dashpot.
9. L. Yang and S. G. Hutton 1995, *Journal of Sound and Vibration*, **185**, 139–154. Interactions between an idealized rotating string and stationary constraints.
10. J. Tian, and S. G. Hutton 1997 *Technical Note*, *ASME Journal of Applied Mechanics*. Lateral vibration instability mechanisms in a constrained rotating string. (in press).

APPENDIX A: TOTAL POWER FLOW

The total power flow $E_{,t}$ in the constrained rotating string system is given by equation (6). Substituting equations (4) and (5) into equation (6) and assuming $\Omega = \text{constant}$ yields

$$E_{,t} = \int_0^{2\pi} (P/r)u_{,\theta}u_{,\theta t}\,\mathrm{d}\theta + \int_0^{2\pi} \rho r(u_{,t} + \Omega u_{,\theta})(u_{,tt} + \Omega u_{,\theta t})\,\mathrm{d}\theta + ku(0,t)u_{,t}(0,t)$$

$$+ mu_{,tt}(0,t)u_{,t}(0,t), \tag{A1}$$

Rearranging equations (A1) gives

$$E_{,t} = \rho r \int_0^{2\pi} \left(\frac{P}{\rho r^2} - \Omega^2\right) u_{,\theta}u_{,\theta t}\,\mathrm{d}\theta + \rho r \int_0^{2\pi} u_{,t}(u_{,tt} + \Omega u_{,\theta t})\,\mathrm{d}\theta$$

$$+ \rho r\Omega \int_0^{2\pi} u_{,\theta}(u_{,tt} + 2\Omega u_{,\theta t})\,\mathrm{d}\theta + [ku(0,t) + mu_{,tt}(0,t)]u_{,t}(0,t)$$

$$= I_1 + I_2 + I_3 + I_4, \tag{A2}$$

where the first term I_1 is

$$I_1 = \rho r \int_0^{2\pi} \left(\frac{P}{\rho r^2} - \Omega^2\right) u_{,\theta}u_{,\theta t}\,\mathrm{d}\theta = \rho r \left(\frac{P}{\rho r^2} - \Omega^2\right)\left(u_{,\theta}u_{,t}|_0^{2\pi} - \int_0^{2\pi} u_{,\theta\theta}u_{,t}\,\mathrm{d}\theta\right).$$

Considering equation (2), the above equation can be rewritten as

$$I_1 = \rho r \left(\frac{P}{\rho r^2} - \Omega^2\right)[u_{,\theta}(2\pi,t) - u_{,\theta}(0,t)]u_{,t}(0,t) - \rho r \left(\frac{P}{\rho r^2} - \Omega^2\right) \int_0^{2\pi} u_{,\theta\theta}u_{,t}\,\mathrm{d}\theta.$$

Substitution of the force boundary condition [equation (3)] yields

$$I_1 = -[ku(0,t) + mu_{,tt}(0,t) + cu_{,t}(0,t) - F_n(0,t)]u_{,t}(0,t)$$
$$-\rho r(P/\rho r^2 - \Omega^2)\int_0^{2\pi} u_{,\theta\theta}u_{,t}\,\mathrm{d}\theta. \tag{A3}$$

The second term in equation (A2) can be rewritten as

$$I_2 = \rho r\int_0^{2\pi} u_{,t}(u_{,tt} + 2\Omega u_{,\theta t})\,\mathrm{d}\theta - \rho r\Omega\int_0^{2\pi} u_{,t}u_{,\theta t}\,\mathrm{d}\theta,$$

where $\int_0^{2\pi} u_{,t}u_{,\theta t}\,\mathrm{d}\theta = u_{,t}^2|_0^{2\pi} - \int_0^{2\pi} u_{,t}u_{,\theta t}\,\mathrm{d}\theta$. Thus

$$\int_0^{2\pi} u_{,t}u_{,\theta t}\,\mathrm{d}\theta = \tfrac{1}{2}[u_{,t}(2\pi,t) - u_{,t}(0,t)][u_{,t}(2\pi,t) + u_{,t}(0,t)] = 0.$$

Substituting the above equation and equation (1) into I_2 leads to

$$I_2 = \rho r\int_0^{2\pi} u_{,t}(P/\rho r^2 - \Omega^2)u_{,\theta\theta}\,\mathrm{d}\theta. \tag{A4}$$

Substituting equations (A3) and (A4) into equation (A2) and simplifying the result, $E_{,t}$ can be expressed as

$$E_{,t} = \rho r\Omega\int_0^{2\pi}\left(\frac{P}{\rho r^2} - \Omega^2\right)u_{,\theta}u_{,\theta\theta}\,\mathrm{d}\theta - [cu_{,t}(0,t) - F_n(0,t)]u_{,t}(0,t), \tag{A5}$$

where $\int_0^{2\pi} u_{,\theta}u_{,\theta\theta}\,\mathrm{d}\theta = u_{,\theta}^2|_0^{2\pi} - \int_0^{2\pi} u_{,\theta}u_{,\theta\theta}\,\mathrm{d}\theta$. Thus $\int_0^{2\pi} u_{,\theta}u_{,\theta\theta}\,\mathrm{d}\theta = \frac{1}{2}[u_{,\theta}^2(2\pi,t) - u_{,\theta}^2(0,t)]$. Substituting into equation (A5), gives

$$E_{,t} = \rho r\Omega\left(\frac{P}{\rho r^2} - \Omega^2\right)[u_{,\theta}(2\pi,t) - u_{,\theta}(0,t)][u_{,\theta}(2\pi,t) + u_{,\theta}(0,t)]/2$$
$$-[cu_{,t}(0,t) - F_n(0,t)]u_{,t}(0,t). \tag{A6}$$

By substituting the force boundary condition [equation (3)] into the above equation, the power $E_{,t}$ can be expressed as

$$E_{,t} = \Omega[-ku(0,t) - mu_{,tt}(0,t) - cu_{,t}(0,t) + F_n(0,t)]\bar{u}_{,\theta}(0,t)$$
$$-[cu_{,t}(0,t) - F_n(0,t)]u_{,t}(0,t) \tag{A7}$$

where $\bar{u}_{,\theta}(0,t) = [u_{,\theta}(2\pi,t) + u_{,\theta}(0,t)]/2$.

Equation (A7) enables a physical explanation of the instabilities that occur in a constrained rotating string system with transverse vibration present.